

Mutagenesis of Residue β Arg-246 in the Phosphate-binding Subdomain of Catalytic Sites of *Escherichia coli* F_1 -ATPase*

Received for publication, April 26, 2004, and in revised form, May 17, 2004
Published, JBC Papers in Press, May 18, 2004, DOI 10.1074/jbc.M404621200

Zulfiqar Ahmad and Alan E. Senior‡

From the Department of Biochemistry and Biophysics, University of Rochester Medical Center, Rochester, New York 14642

Residues responsible for phosphate binding in F_1F_0 -ATP synthase catalytic sites are of significant interest because phosphate binding is believed linked to proton gradient-driven subunit rotation. From x-ray structures, a phosphate-binding subdomain is evident in catalytic sites, with conserved β Arg-246 in a suitable position to bind phosphate. Mutations β R246Q, β R246K, and β R246A in *Escherichia coli* were found to impair oxidative phosphorylation and to reduce ATPase activity of purified F_1 by 100-fold. In contrast to wild type, ATPase of mutants was not inhibited by MgADP-fluoroaluminate or MgADP-fluoroscandium, showing the Arg side chain is required for wild-type transition state formation. Whereas 7-chloro-4-nitrobenzo-2-oxa-1,3-diazole (NBD-Cl) inhibited wild-type ATPase essentially completely, ATPase in mutants was inhibited maximally by ~50%, although reaction still occurred at residue β Tyr-297, proximal to β Arg-246 in the phosphate-binding pocket. Inhibition characteristics supported the conclusion that NBD-Cl reacts in β E (empty) catalytic sites, as shown previously by x-ray structure analysis. Phosphate protected against NBD-Cl inhibition in wild type but not in mutants. The results show that phosphate can bind in the β E catalytic site of *E. coli* F_1 and that β Arg-246 is an important phosphate-binding residue.

ATP synthesis from ADP and P_i in oxidative and photophosphorylation occurs in the catalytic sites of F_1F_0 -ATP synthase. This membrane enzyme uses the energy of an ion gradient (usually protons) to drive rotation of a “rotor” composed of subunits $\gamma\epsilon_n$ (where n can vary from 10 to 14 in different organisms), the rotor serving as a transmission device which upon rotation drives the chemical synthesis of ATP sequentially at three catalytic sites. Catalytic sites are located at α/β interfaces of the $\alpha_3\beta_3$ subunit hexagon, which are immobilized during rotation by the “stator,” consisting of subunits δb_2 . The proton motor is composed of the single a and a ring of c subunits. Experimental work in this system has been greatly facilitated by the ability to separate the water-soluble F_1 sector (subunits $\alpha_3\beta_3\gamma\delta\epsilon$) from the membrane-embedded F_0 sector (subunits ab_2c_{ring}), with retention of ATP hydrolysis function in the former and of proton conduction in the latter. For recent reviews of structure and function of ATP synthase see Refs. 1–4.

* This work was supported by National Institutes of Health Grant GM25349 (to A. E. S.). The costs of publication of this article were defrayed in part by the payment of page charges. This article must therefore be hereby marked “advertisement” in accordance with 18 U.S.C. Section 1734 solely to indicate this fact.

‡ To whom correspondence should be addressed: Dept. of Biochemistry and Biophysics, Box 712, University of Rochester Medical Center, Rochester, NY 14642. Tel.: 585-275-6645; Fax: 585-271-2683; E-mail: alan_senior@urmc.rochester.edu.

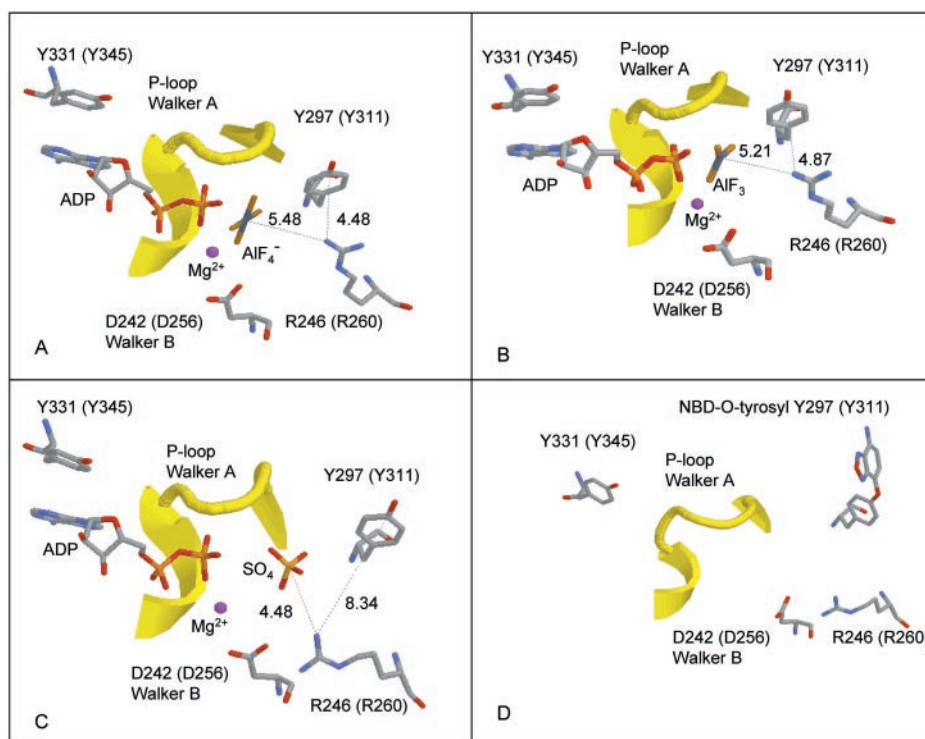
Based on kinetic measurements, Boyer and co-workers (5, 6) hypothesized that the affinity of catalytic sites for P_i is increased by the proton gradient, and currently the concept that P_i binding is enhanced by proton gradient-driven subunit rotation appears well supported. Significant P_i binding to *Escherichia coli* F_1 catalytic sites was not measurable by direct binding assay using radioactive P_i (7). The K_d value for P_i binding was >10 mM as measured by competition with Mg-AMPPNP or ATP in fluorescence titrations using the β Y331W mutant enzyme (8–10). Calculations based on unisite catalysis kinetics showed that K_dP_i in unisite catalysis is 2.3×10^3 M in *E. coli* and 87 M in mitochondrial F_1 (11). Although not directly applicable to physiological catalysis (2), such calculations underline the weak affinity that the catalytic site of highest affinity for ATP has for P_i in the absence of proton-driven rotation. On the other hand, measurements of K_mP_i for ATP synthesis are in the range of ~1 mM (12–14). An important conclusion is that P_i binding and release steps are likely to be intimately linked to rotational movements of subunits (1, 2, 15).

An often overlooked but crucial question in the mechanism of ATP synthesis is, how does the enzyme bind ADP plus P_i and not ATP into catalytic sites? In active cells the cytoplasmic concentrations of ATP and P_i are approximately in the 2–5 mM range, whereas that of ADP is at least 10–50-fold lower. Equilibrium binding assays have established that both ADP and ATP bind to catalytic sites of purified F_1 and detergent-solubilized F_1F_0 with relatively similar binding affinities (8, 9, 16, 17). Obviously, the enzyme must have evolved a specific mechanism for selectively binding ADP into catalytic sites while contemporaneously discouraging access of ATP during proton-driven rotation and ATP synthesis. One hypothesis is that during ATP synthesis, proton gradient-driven rotation of subunits drives an empty catalytic site to bind P_i tightly, thus stereochemically precluding ATP binding and therefore selectively favoring ADP binding (18). Further understanding of features that determine P_i binding is therefore of major importance in formulating a mechanism for ATP synthesis. So far, none of the residues directly involved in binding P_i has been identified experimentally.

X-ray structural analysis has indicated the possible location of the P_i binding subdomain in the catalytic sites. A residue within this subdomain that could be significantly involved in P_i binding is β Arg-246¹ (equivalent to β Arg-260 in mitochondrial F_1), conserved in all known species. Fig. 1A shows ADP·AlF₄⁻ bound in the β DP catalytic site (19) in what is believed to be a transition state analog structure. Fig. 1B shows the β DP site with ADP and AlF₃ bound in what is believed to be a late transition state or early ground state structure (20), and Fig. 1C shows the β ADP + P_i site (also called the “half-closed” or

¹ *E. coli* residue numbers used throughout.

FIG. 1. X-ray structures of catalytic sites in mitochondrial F_1 -ATPase. *A*, the β DP site in the AlF_4^- -inhibited enzyme (19). Residue numbers correspond to *E. coli* numbering, with mitochondrial numbering in parentheses. Distances are given in Angstroms. *B*, the β DP site in the AlF_3 -inhibited enzyme (20). *C*, the β ADP + P_i (" β -half-closed") site in the AlF_4^- -inhibited enzyme (19). The sulfate ion is thought to occupy the position of natural P_i . β Arg-246 has rotated such that atom NH1 is now closest to the sulfate ion, whereas in *A* and *B*, atom NH₂ was closest to the Al atom. *D*, reacted NBD-*O*-tyrosyl-297 in the β E site (47).



β HC site) in what is believed to be a post-hydrolysis state (19). In this latter site, an SO_4^{2-} ion is present which is thought to mimic phosphate, whereas in Fig. 1, *A* and *B*, fluoroaluminate is in the position of the phosphate. In Fig. 1, *A*–*C*, residue β Arg-246 lies close to the phosphate moiety, at the end of what appears to be a phosphate-binding pocket also demarcated by residue β Tyr-297. The distance between the phosphate moiety and β Arg-246 changes decrementally as the transition state collapses to the post-hydrolysis state. Moreover Fig. 1, *A*–*C*, suggests experimental approaches to determine whether β Arg-246 is an important determinant of P_i binding, namely the use of surrogates for P_i or the γ -P of ATP, such as fluoroaluminate, fluoroscandium, and fluoroberyllate, or the use of NBD-Cl² which reacts specifically with residue β Tyr-297, located at the end of the P_i binding subdomain (Fig. 1*D*).

Early random mutagenesis experiments revealed that mutations β R246H and β R246C impaired oxidative phosphorylation drastically and reduced ATPase activity in purified F_1 to ~1% of wild type (21, 22). Later work showed that unisite catalysis parameter K_dP_i was changed by 4 orders of magnitude, whereas K_dADP was largely unaltered by β R246C, and the ATP hydrolysis reaction equilibrium constant changed to favor ATP over ADP plus P_i (11). Recent computer simulations have drawn attention to β Arg-246. Movement of the residue during rotation, change of the conformation of the sites (23), and a role in liganding P_i and the transition state were predicted (24, 25).

The goal of this paper was to determine experimentally whether residue β Arg-246 does in fact contribute to P_i binding in ATP synthase catalytic sites. We used site-directed mutagenesis to substitute Gln, Lys, and Ala for residue β Arg-246, and we have examined the effects of each mutation on function. A variety of inhibitors and ligands known to bind or react in the catalytic sites close to the P_i -binding subdomain was utilized in combination with the mutant enzymes to establish the role of the β Arg-246 side chain.

EXPERIMENTAL PROCEDURES

Preparation of E. coli Membranes; Purification of F_1 ; Measurement of Growth Yield in Limiting Glucose Medium; Assay of ATPase Activity of Membranes or Purified F_1 —E. coli membranes were prepared as described previously (26). Prior to the experiments, membranes were washed twice by resuspension and ultracentrifugation in 50 mM TrisSO₄, pH 8.0, 2.5 mM MgSO₄. F_1 was purified as in Ref. 27. Prior to the experiments, F_1 samples (100 μ l) were passed twice through 1-ml centrifuge columns (Sephadex G-50) equilibrated in 50 mM TrisSO₄, pH 8.0, to remove catalytic site-bound nucleotide. Growth yield in limiting glucose was measured as described previously (28). ATPase activity was measured in 1 ml of assay buffer containing 10 mM NaATP, 4 mM MgCl₂, 50 mM TrisSO₄, pH 8.5. Specific activity was measured at 30 °C, and measurements of inhibition by inhibitors were done at room temperature. Reactions were started by addition of enzyme and stopped by addition of SDS to 3.3% final concentration. P_i released was assayed as described previously (29). For wild-type membranes and F_1 , reaction times were 2–10 min. For mutant enzymes reaction times were 30–120 min. All reactions were shown to be linear with time and protein concentration.

E. coli Strains—For purified F_1 , wild-type strain SWM1 was used (30), and for membranes wild type was pBWU13.4/DK8 (31). For fluorescence titrations with purified F_1 , strain SWM4 (β Y331W) (8) was used as the "wild type." Mutant strains were β R246Q/ β Y331W, β R246K/ β Y331W, and β R246A/ β Y331W, all three in DK8 and constructed as indicated below.

Construction of Mutant Strains of E. coli—pSN6 is a plasmid containing the β Y331W mutation from plasmid pSWM4 (8) introduced on a SacI-EagI fragment into pBWU13.4 (31) which expresses all the ATP synthase genes. The template for oligonucleotide-directed mutagenesis was M13mp18 containing the HindIII-XbaI fragment from pSN6. Mutagenesis was by the method of Vandeyar *et al.* (32). Mutagenic oligonucleotides were as follows: for β R246Q, GACAACATCTATCAGTATAC-CCTGGCCGG, where the underlined bases introduce the mutation and a new BstII107I restriction site; for β R246K, GACAACATCTATAAGTAT-ACCCTGGCCGG, where the underlined bases introduce the mutation and a new BstII107I restriction site; and for β R246A, GACAACATCTAT-GCATACACCCTGGC, where the underlined bases introduce the mutation site and a new NsiI restriction site. DNA sequencing was performed to confirm the presence of mutations and absence of undesired changes in sequence, and the mutations were transferred to pSN6 on SacI-EagI fragments, generating the new plasmids pZA5 (β R246Q/ β Y331W), pZA6 (β R246K/ β Y331W), and pZA7 (β R246A/ β Y331W), respectively. Each plasmid was transformed into strain DK8 (33) containing a deletion of ATP synthase genes for expression of the mutant enzymes.

² The abbreviations used are: NBD-Cl, 7-chloro-4-nitrobenzo-2-oxa-1,3-diazole; DTT, dithiothreitol; AMPPNP, adenosine 5'-(β , γ -imino)triphosphate.

TABLE I
Effects of *βArg-246* mutations on cell growth and *F₁-ATPase* activity

Mutation ^a	Growth on succinate	Growth yield in limiting glucose	ATPase activity of purified F ₁
	+ / -	%	<i>μmol/min/mg</i>
Wild-type	+++	100	28
Null	-	42	
<i>βY331W</i> alone	+++	93	14
<i>βR246Q</i>	-	48	0.27
<i>βR246K</i>	-	50	0.27
<i>βR246A</i>	-	50	0.25

^a Wild-type, pBWU13.4/DK8; Null, pUC118/DK8. All three *βArg-246* mutants were expressed with the *βY331W* mutation also present.

Fluorescence Titrations—The method utilizes the quench of fluorescence of introduced residue *βTrp-331* that occurs upon nucleotide binding to catalytic sites (34). Titration with MgADP and MgATP was carried out in 50 mM TrisSO₄, pH 8.0, 2.5 mM MgSO₄ at room temperature. NaADP and NaATP were added incrementally. Excitation was at 295 nm, and emission was at 360 nm in a SPEX Fluorolog 2 spectrofluorometer. Final enzyme concentration in the cuvette was 150–200 nM, and enzyme was incubated for 10 min at room temperature before titration was begun. Background signals due to buffer were subtracted, and volume and inner filter effects were corrected by carrying out parallel titrations with wild-type F₁. Calculation of nucleotide binding parameters was accomplished by fitting theoretical curves to the measured data points assuming models with three types of binding sites (34, 35).

Inhibition of ATPase Activity—For fluoroaluminate, fluoroscandium, fluoroberyllate, and vanadate inhibition, F₁ was incubated for 60 min at room temperature in 50 mM TrisSO₄, 2.5 mM MgSO₄, 1 mM NaADP, and 10 mM NaF at a protein concentration of 0.2–1.0 mg/ml in presence of AlCl₃, ScCl₃, or BaSO₄, added at varied concentrations (see “Results”). 100-*μl* aliquots were then added to 1 ml of ATPase assay buffer, and activity was measured as above. It was confirmed in control experiments that no inhibition was seen if MgSO₄, NaADP, or NaF was omitted. NaF was absent when vanadate was the inhibitor, and sodium orthovanadate was pretreated as described (36). For NBD-Cl inhibition of purified F₁, NBD-Cl was prepared as a stock solution in dimethyl sulfoxide and protected from light. Enzyme (0.2–0.4 mg/ml) was reacted with NBD-Cl for 60 min in the dark, at room temperature, in 50 mM TrisSO₄, pH 8.0, 2.5 mM MgSO₄, and then 100-*μl* aliquots were transferred to 1 ml of ATPase assay buffer to determine activity. For NBD-Cl inhibition of F₁F₀ in membranes, protein concentration was 0.7–1.0 mg/ml in 50-*μl* aliquots; the other conditions were the same. Where protection from NBD-Cl inhibition by ADP or P_i was determined, F₁ and membranes were preincubated for 60 min with protecting agent before addition of NBD-Cl. MgSO₄ was present, equimolar with ADP or P_i. Control samples containing the ligand without added NBD-Cl were included. Neither P_i (up to 50 mM) nor MgADP (up to 10 mM) had any inhibitory effect alone. For measurement of azide inhibition, sodium azide at varied concentrations was added directly to the ATPase assay buffer, to which F₁ was added to start the reaction.

RESULTS

Properties of *βR246Q*, *βR246K*, and *βR246A* Mutants of *E. coli* ATP Synthase—Residue *βArg-246* was changed to Gln, Lys, or Ala by oligonucleotide-directed mutagenesis, and then the mutant ATP synthase complex was expressed from a plasmid in a strain of *E. coli* (DK8) containing a deletion of the ATP synthase genes. It should be noted that the additional mutation *βY331W* was also present in all three cases, to allow monitoring of nucleotide binding affinity and stoichiometry in purified F₁ by fluorescence titration. Effects of the *βArg-246* mutations on oxidative phosphorylation *in vivo* were assayed by growth on succinate-containing plates and in limiting glucose medium. All three mutations prevented growth on succinate. Growth yields on limiting glucose were reduced close to the ATP synthase null control (Table I). Therefore, all three mutations seriously impaired ATP synthesis *in vivo*. The *βY331W* mutation alone has little effect on growth.

F₁ was purified from each mutant, and yields were similar to that with wild-type enzyme. On SDS gels, the enzymes ap-

TABLE II
MgATP and MgADP binding parameters of mutant enzymes
K_d values are given in *μM*.

	<i>βY331W</i> ^a	<i>βR246Q</i>	<i>βR246K</i>	<i>βR246A</i>
MgADP				
<i>K_{d1}</i>	0.04	0.28	1.03	0.07
<i>K_{d2}</i>	1.8	9.2	24.9	2.8
<i>K_{d3}</i>	34.8	34.0	61.1	16.5
MgATP				
<i>K_{d1}</i>	0.02	0.32	0.56	0.10
<i>K_{d2}</i>	1.4	5.2	32.6	2.2
<i>K_{d3}</i>	23.0	28.6	33.4	37.8

^a Values were taken from Ref. 34. Similar values were obtained in this work.

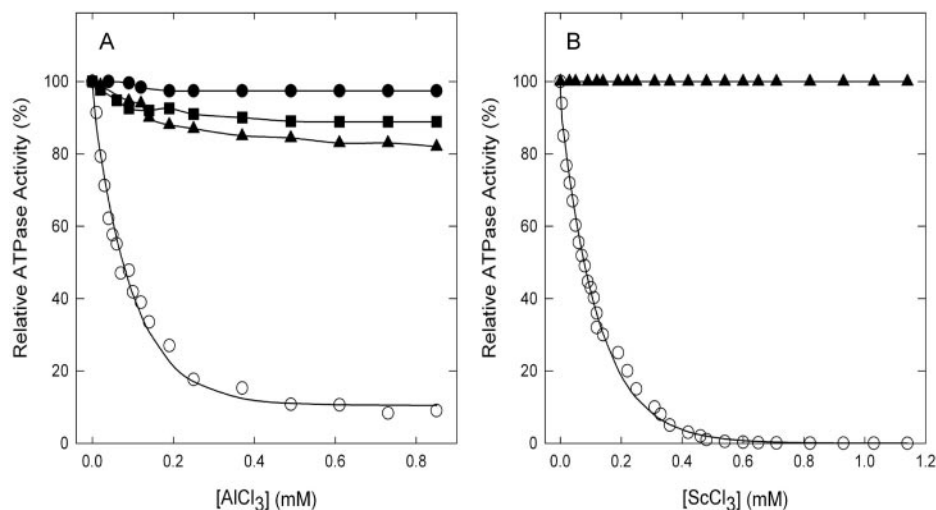
peared pure and showed the same subunit composition as in wild type. Analysis of Trp content by measurement of fluorescence in 6 M guanidine hydrochloride (*λ_{exc}* = 295 nm, *λ_{em}* = 360 nm) confirmed that the purity of the mutant enzymes was the same as wild type, with the expected 12 Trp/mol. Specific ATPase activities for the mutant enzymes are given in Table I. The ATPase activity was around 1% of wild type in all three mutant enzymes. Similar activity had been seen earlier in *βR246H* and *βR246C* enzymes (21, 22). Retention of the positive charge in the *βR246K* mutant did not therefore affect the outcome of mutagenesis, at least as far as ATPase activity *in vitro* or ATP synthesis *in vivo* were concerned.

Ability of the Mutant F₁ to Bind MgATP and MgADP—Fluorescence of introduced residue *βTrp-331* was used to measure MgATP binding characteristics (8, 34). Titrations of the purified mutant F₁ enzymes with the nucleotides were carried out (data not shown), and *K_d* values for binding at each of the three catalytic sites, calculated as described under “Experimental Procedures,” are listed in Table II. The mutations caused reduction of affinity for MgATP, most noticeably at site two (the site of “medium” affinity) and at site one (highest affinity) with little effect at site three (lowest affinity). Most interesting, the mutation that might have been predicted to have the smallest effect, namely *βR246K*, in fact had the largest effect. With MgADP there was again loss of affinity at sites one and two, with lesser effects at site three, and the *βR246K* mutant had the largest effect. It appears, however, that the large effects of the mutations on ATP synthesis and ATPase activity are not commensurately reflected in impairment of substrate ADP or ATP binding affinities. At saturation (1 mM of MgADP or MgATP) all three mutant enzymes would contain all three sites filled, as in wild type.

Inhibition of ATPase Activity of F₁ by Phosphate Analogs Fluoroaluminate, Fluoroscandium, Orthovanadate, and Fluoroberyllate—Wild-type or *βY331W E. coli* F₁-ATPase is strongly inhibited by AlCl₃ in combination with NaF, ADP, and Mg²⁺ (37, 38), and experiments showed that MgADP-fluoroaluminate formed a tenaciously bound inhibitory complex with F₁ that mimicked a transition state (38–40). X-ray crystallography subsequently deduced the structure of mitochondrial F₁ with both ADP·AlF₃ and ADP·AlF₄⁻ species bound (19, 20). Fig. 2A shows that the mutations *βR246Q*, *βR246K*, or *βR246A* all rendered *E. coli* F₁ insensitive to ADP·fluoroaluminate inhibition. Since the concentration of MgADP in these experiments (1 mM) was easily sufficient to saturate the enzyme catalytic sites (Table II), our conclusion is that substitution of *βArg-246* greatly weakens interaction with the fluoroaluminate moiety. Notably, even the Lys mutant was unable to substitute for Arg.

MgADP-fluoroscandium complex was also shown to inhibit wild-type and *βY331W F₁-ATPase* activity potently (41) by mimicking a transition state. Fig. 2B shows that the mutants *βR246Q*, *βR246K*, and *βR246A* were all completely immune to ADP-fluoroscandium inhibition, again suggesting that *βArg-*

FIG. 2. Inhibition of purified F_1 from mutant and wild-type enzymes by fluoroalumininate and fluoroscandium. A, inhibition of ATPase after preincubation for 60 min with 1 mM MgADP, 10 mM NaF, and varied $AlCl_3$. B, inhibition of ATPase after preincubation for 60 min with 1 mM MgADP, 10 mM NaF, and varied $ScCl_3$. \circ , wild type; \bullet , $\beta R246Q/\beta Y331W$; \blacksquare , $\beta R246K/\beta Y331W$; \blacktriangle , $\beta R246A/\beta Y331W$. B, all three mutants showed the same behavior, and only one is shown for clarity.



246 in wild type is normally important in liganding the fluoroaluminum moiety and bringing about inhibition.

MgADP-vanadate complex is an inhibitory transition state analog that has been used to study a variety of ATPase enzymes. Because the vanadate moiety is pentavalent in the inhibited enzyme complex (e.g. Ref. 42), ADP-vanadate is thought to provide a close mimic of a true transition state of a natural transphosphorylation reaction (43). Unfortunately, both wild-type and mutant *E. coli* F_1 proved to be resistant to inhibition by vanadate (up to 2.4 mM) in combination with 1 mM MgADP (data not shown).

The MgADP-fluoroberyllate complex is different from the preceding inhibitors in that the bound complex mimics a ground state with ATP bound (e.g. Ref. 44). MgADP-fluoroberyllate is a potent inhibitor of wild-type *E. coli* F_1 as shown in Fig. 3. Here a varied pattern of inhibition was seen with the mutant enzymes. $\beta R246K$ was inhibited to the same extent as wild type (~90%); $\beta R246A$ was inhibited by ~45% and $\beta R246Q$ by ~30%. Thus, substitution of Arg impaired liganding to the fluoroberyllate moiety in Ala and Gln mutants but not with Lys.

To summarize, the results show that residue β Arg-246 is critical for liganding the phosphate moiety of ATP in the transition state and that it also plays a role in binding the γ -P in the MgADP-fluoroberyllate complex. Lys can substitute in the latter situation but not in the former.

Inhibition of ATPase Activity of F_1 by Azide—Azide is a potent inhibitor of F_1 -ATPases in general, although its mode of inhibition remains controversial (45). It has not yet been located in x-ray structures of F_1 . One school of thought envisages that azide might form a tightly bound MgADP· N_3^- complex at catalytic site(s) (46). However, data in Ref. 45 led to the conclusion that azide blocks conformational signal transmission between catalytic sites. Fig. 4 shows that the mutant $\beta R246Q$, $\beta R246K$, and $\beta R246A$ enzymes were all remarkably resistant to inhibition by sodium azide (note that $\beta Y331W$ F_1 is strongly inhibited by azide, see Ref. 45).

Inhibition of ATPase Activity of Purified F_1 and F_1F_0 in Membranes by NBD-Cl in β Arg-246 Mutants—NBD-Cl is a potent inhibitor of F_1 -ATPase activity that covalently reacts at a stoichiometry of 1 mol/mol F_1 , specifically with residue β Tyr-297, situated at the end of the P_i binding pocket and very close to β Arg-246 (Fig. 1, A-C). Fig. 1D shows x-ray structure analysis of the empty catalytic site (βE) containing the covalent NBD-*O*-tyrosyl adduct (47). Our interest in NBD-Cl inhibition was piqued not only because residue β Tyr-297 is close to β Arg-246 and to the P_i moiety in catalytic sites but also because Perez *et al.* (48) had reported that P_i protects against NBD-Cl

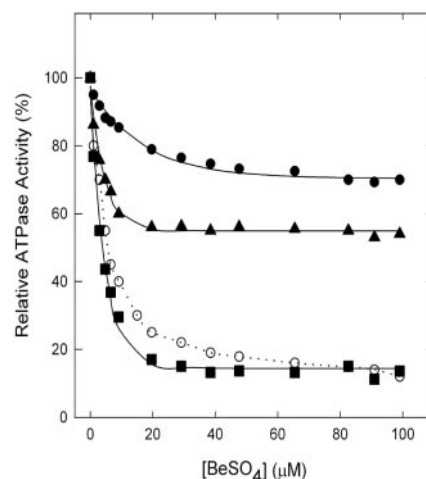


FIG. 3. Inhibition of purified F_1 from mutant and wild-type enzymes by fluoroberyllate. Inhibition of ATPase after preincubation for 60 min with 1 mM MgADP, 10 mM NaF, and varied $BeSO_4$. \circ , wild type; \bullet , $\beta R246Q/\beta Y331W$; \blacksquare , $\beta R246K/\beta Y331W$; \blacktriangle , $\beta R246A/\beta Y331W$.

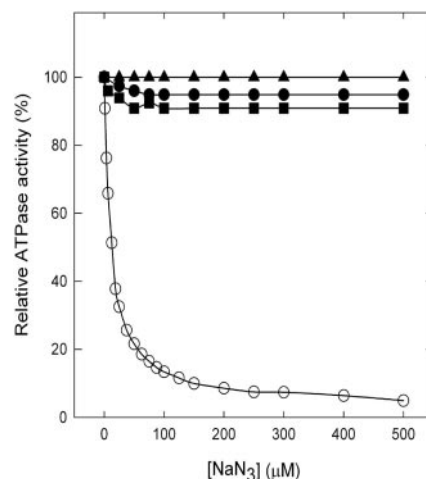


FIG. 4. Inhibition of purified F_1 from mutant and wild-type enzymes by azide. Sodium azide was added directly to the ATPase assay buffer at concentration shown. \circ , wild type; \bullet , $\beta R246Q/\beta Y331W$; \blacksquare , $\beta R246K/\beta Y331W$; \blacktriangle , $\beta R246A/\beta Y331W$.

inhibition of F_1F_0 -ATPase in mitochondrial membrane preparations, potentially providing a tool to assess the role of β Arg-246 in P_i binding.

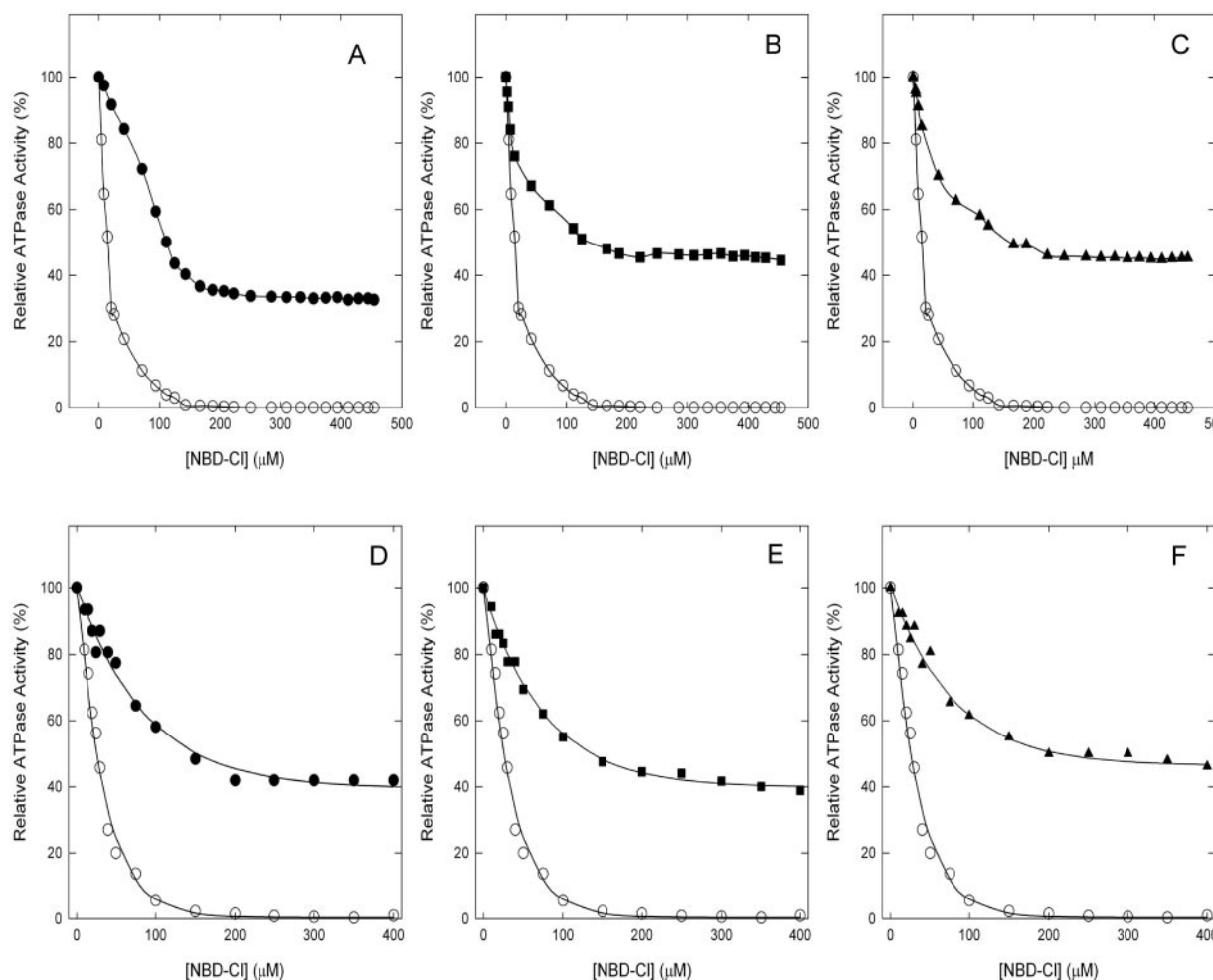


FIG. 5. Inhibition of purified F_1 and membrane-bound F_1F_0 by NBD-Cl. Enzyme was preincubated for 60 min at 23 °C with the indicated concentration of NBD-Cl, then aliquots were added to 1 ml of assay buffer, and ATPase activity was determined. For details see “Experimental Procedures.” ○, wild type; ●, β R246Q/ β Y331W; ■, β R246K/ β Y331W; ▲, β R246A/ β Y331W. A–C, purified F_1 ; D–F, membrane-bound enzyme.

Initial experiments revealed an interesting difference between mutants and wild type, which was that the former showed only ~50% inactivation by NBD-Cl both in purified F_1 (Fig. 5, A–C) or in membranes (Fig. 5, D–F), whereas wild type was almost totally inactivated (we confirmed that β Y331W alone behaved the same as wild type). With the mutant enzymes, approximately the same degree of residual ATPase activity remained in purified F_1 as in membranes. It may be noted that NBD-Cl was extremely effective in wild type, with residual ATPase activity amounting to only 0.02 μ mol/min/mg of purified F_1 protein at the higher concentrations of NBD-Cl, whereas residual activities in the mutant purified F_1 enzymes were around 0.10–0.12 μ mol/min/mg. Inhibition with NBD-Cl was independent of the presence of $MgSO_4$ in the reaction buffer. Maximal inhibition was reached in 1 h at room temperature with 150 μ M NBD-Cl in the mutant purified F_1 (Fig. 5, A–C). If at the end of this period, an additional pulse of NBD-Cl equivalent to extra 200 μ M was added and incubation was continued for an additional hour, little additional inhibition occurred (Fig. 6A). Thus the reason for incomplete inhibition in the mutant enzymes in Fig. 5 was that the fully reacted enzymes retained significant residual activity, whereas in wild type residual activity was negligible. It is notable that all three mutant enzymes behaved similarly. Therefore, it appears that mutation of β Arg-246 affected both reactivity of the proximal residue β Tyr-297 with NBD-Cl and the level of residual ATPase in the fully reacted enzyme. Incubation with 4 mM DTT

after maximal inhibition had been achieved restored full activity in all cases (Fig. 6B), establishing that the reaction was specifically with residue β Tyr-297 in the mutant enzymes (49, 50).

Inhibition of ATPase Activity by NBD-Cl in Membranes and Purified F_1 ; Protection by MgADP and P_i —Orriss et al. (47) concluded that NBD-Cl reacts only in the empty (β E) catalytic site, and that it does not act as a nucleotide analog based on the location of the derivatized Tyr residue in the x-ray structure. This was supported here by the following two lines of evidence. First it was found that the pseudo-first order rate constant for inhibition (k_{obs}) was linearly dependent upon NBD-Cl concentration (data not shown), implying that no initial binding event was required (which would yield a hyperbolic dependence of k_{obs} on concentration). Second, it was found that MgADP protected purified F_1 and F_1F_0 in membranes from reaction with NBD-Cl, but only at extremely high concentrations that would effectively keep the third site (β E) occupied in time average and thus impede access to NBD-Cl by closing (or “half-closing”) the site. Fig. 7 shows data for MgADP protection against NBD-Cl in purified F_1 and membrane enzymes. Wild-type and all three mutant enzymes were protected by MgADP against NBD-Cl inhibition, with similar EC_{50} values of 3–5 mM. Control experiments in which MgADP was preincubated with purified or membrane-bound F_1 in the absence of NBD-Cl showed no inhibition of ATPase activity, up to 10 mM MgADP. Above this concentration inhibition began to occur, presumably as a result

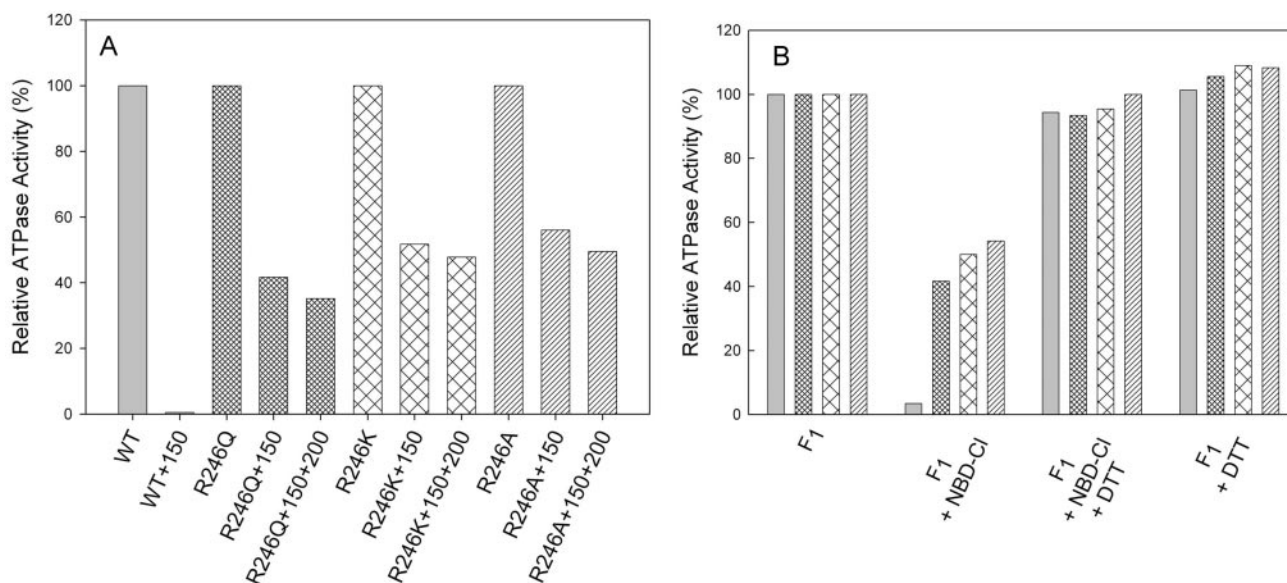


FIG. 6. Results of an extra pulse of NBD-Cl in mutant enzymes and reversal of NBD-Cl inhibition by DTT. A, purified F_1 was inhibited by reaction with $150 \mu\text{M}$ NBD-Cl for 60 min under conditions as described in Fig. 5. Then a further pulse of NBD-Cl, equivalent to $200 \mu\text{M}$, was added and incubation continued a further 60 min before assay. B, purified F_1 was incubated with or without $150 \mu\text{M}$ NBD-Cl for 60 min as in Fig. 5. Degree of inhibition was assayed. In parallel samples, DTT (4 mM) was then added, and incubation continued for a further 60 min before assay. In each group of histograms, the order is, from left to right, wild type, β R246Q, β R246K, and β R246A.

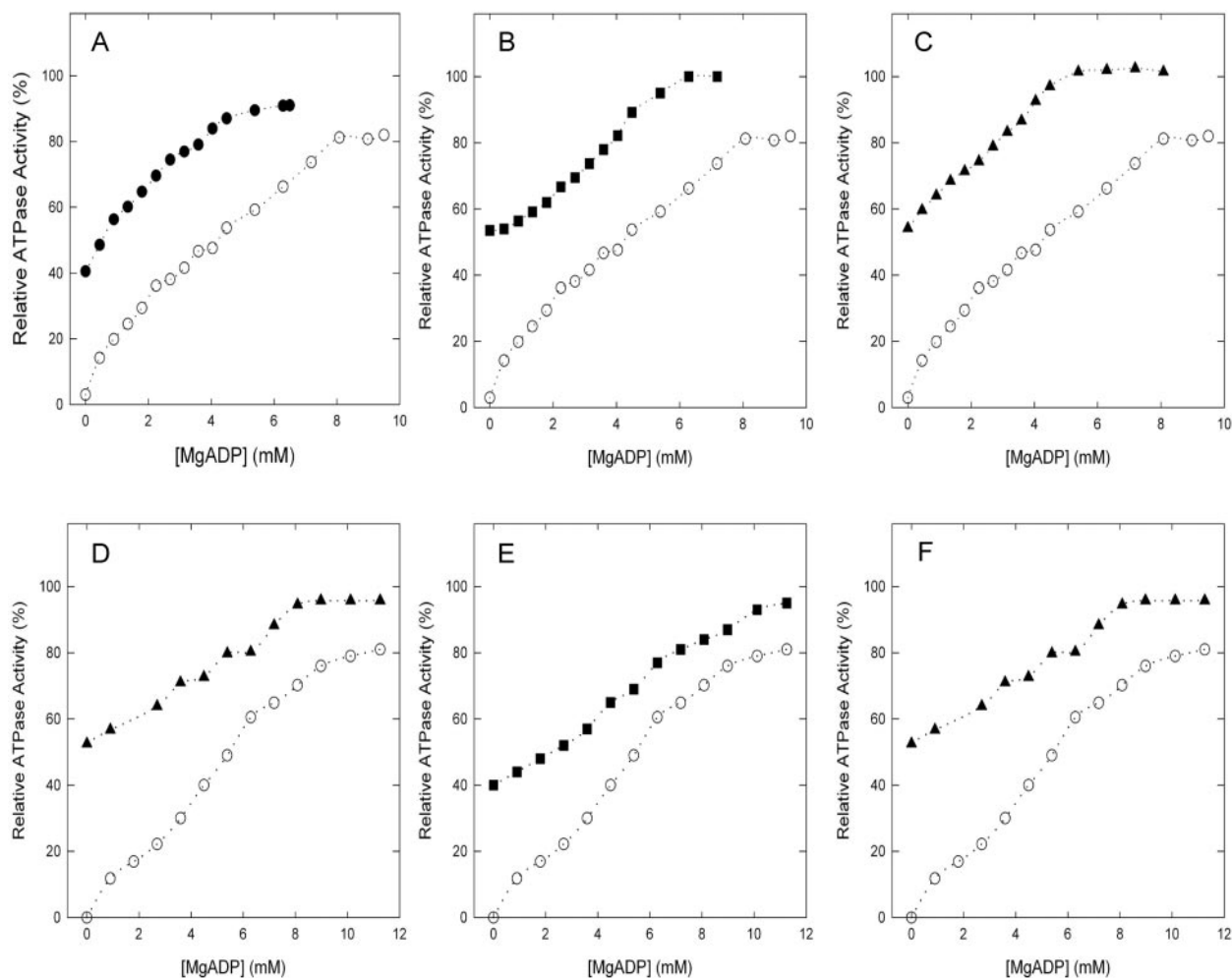


FIG. 7. MgADP protection of ATPase activity in wild type and mutant purified F_1 and membranes from inactivation by NBD-Cl. Purified F_1 or membranes were preincubated with varying concentrations of MgADP for 60 min at 23°C , and then NBD-Cl ($100 \mu\text{M}$) was added and incubation continued for 60 min at the end of which ATPase activity was assayed. For further details see "Experimental Procedures." ○, wild type; ●, β R246Q/ β Y331W; ■, β R246K/ β Y331W; ▲, β R246A/ β Y331W. A-C, purified F_1 ; D-F, membrane-bound enzyme.

FIG. 8. **Protection by P_i of wild-type ATPase activity in membranes and purified F_1 from inactivation by NBD-Cl.** Membranes or purified F_1 were preincubated with P_i at 2.5 or 10 mM concentration as shown for 60 min at 23 °C. Then NBD-Cl (100 μ M) was added, and aliquots were withdrawn for assay at the time intervals as shown. ATPase activity remaining is plotted against time of incubation with NBD-Cl. *A*, wild-type membranes. *B*, wild-type purified F_1 . \circ , no P_i added; \square , 2.5 mM P_i ; \triangle , 10 mM P_i .

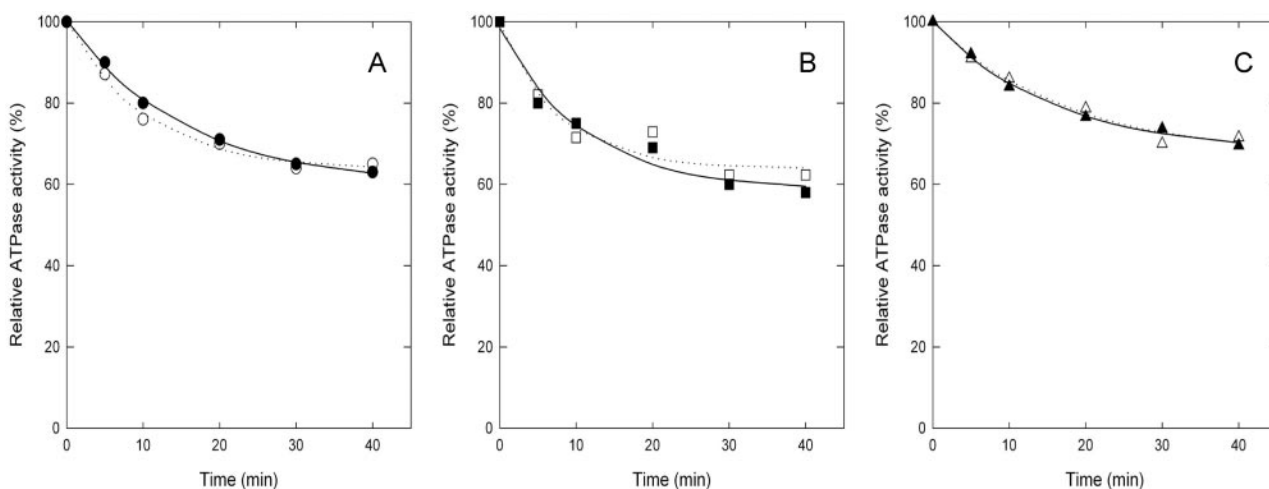
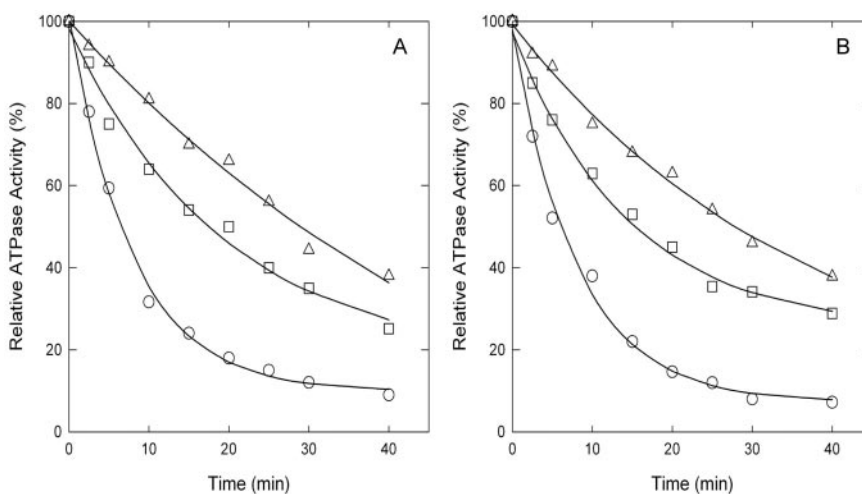


FIG. 9. **Protection by P_i of mutant ATPase activity in membranes from inactivation by NBD-Cl.** The procedure was as in Fig. 8. *Solid symbols* have no P_i added. \bullet , β R246Q/ β Y331W; \blacksquare , β R246K/ β Y331W; \blacktriangle , β R246A/ β Y331W. *Open symbols* have 10 mM P_i added. \circ , β R246Q/ β Y331W; \square , β R246K/ β Y331W; \triangle , β R246A/ β Y331W. The same results were seen with 2.5 mM P_i .

of carryover of MgADP into the ATPase assay.

Perez *et al.* (48) found that P_i protected F_1F_0 -ATPase activity in mitochondrial membranes from inhibition by NBD-Cl. In initial experiments here with wild-type enzyme in *E. coli* membranes, or with purified F_1 , we found that if P_i (up to 10 mM) was preincubated with enzyme under conditions used to study MgADP protection as in Fig. 7 (*i.e.* all samples reacted 60 min with 100 μ M NBD-Cl), then the maximum degree of protection seen with P_i in wild type was around 25%, and no protection was seen in the mutants. Perez *et al.* (48), however, used a different experimental approach in which inactivation by NBD-Cl was monitored as a function of time in the absence or presence of P_i . When we used this approach on wild-type *E. coli* membranes or purified F_1 , protection by P_i was evident (Fig. 8). Moreover, no protection was seen with any of the mutants when membrane enzyme was tested (Fig. 9). It was also found that P_i showed no protection in purified mutant F_1 (data not shown).

DISCUSSION

The goal of this work was to examine the functional role(s) of residue β Arg-246 of *E. coli* ATP synthase. This residue is located in the phosphate-binding pocket of the catalytic sites (Fig. 1). P_i binding and release are important steps in ATP synthase mechanism, likely coupled to rotational movement of subunits, and from its location β Arg-246 could be directly involved. However there is little previous experimental evidence

available on the role of this residue. Here we mutated the Arg side chain to Gln (removes charge, preserves bulk), Lys (preserves positive charge), and Ala (removes side chain and charge).

All three mutations had the same effect on function, namely growth by oxidative phosphorylation was severely impeded, and ATPase activity of purified F_1 was \sim 1% of wild type. Previous work on β R246H and β R246C mutants had given the same results. The first conclusion therefore is that the Arg side chain at this location is critical for function. MgATP and MgADP binding parameters were determined by fluorescence titration. The mutants showed lower affinity for MgATP at the first two catalytic sites, and most interesting, the β R246K mutation produced the largest effect, despite retaining the positive charge. The Ala mutant was least affected. The same pattern was seen for MgADP binding, where deviations from wild type were smaller. From these data it is apparent that the positive charge on β Arg-246 is not critical for nucleotide substrate or product binding. Whereas the mutations did produce lessening of MgATP binding affinity, to differing extents, this was not well correlated with impairment of ATPase.

Fluoroaluminate and fluoroscandium in combination with ADP and Mg^{2+} ions inhibit wild-type *E. coli* F_1 potently and have been shown to increase greatly the affinity for ADP binding at two of the three catalytic sites (38, 41). Both are believed to mimic the chemical transition state, and indeed transition

state-like structures involving the bound $\text{MgADP}\cdot\text{AlF}_4^-$ complex were seen in two catalytic sites by x-ray crystallography (19). Here we found that inhibition by these compounds was abrogated by the β Arg-246 mutations, showing that the Arg side chain is critical for binding the analogs. Apparently the transition state that forms in the mutants is different from normal in that coordination of the γ -P is altered. This is consistent with a previously stated conclusion (51) that "mutant β R246C seemed to have a different multisite reaction pathway." Thus β Arg-246 is critical for formation of wild-type transition state and the rapid catalysis that ensues.

Fluoroberyllate in combination with MgADP is usually regarded as a ground state analog of the substrate ATP in transphosphorylation reactions (44, 52, 53). It is a potent inhibitor of wild-type *E. coli* F_1 -ATPase as shown in Fig. 3. Surprisingly, the three mutations had quite different effects on inhibition as seen in Fig. 3, and these effects were not correlated with effects on MgATP binding (Table II). β R246K retained full inhibition, whereas β R246Q and β R246A reduced it to different degrees. Apparently, MgADP·BeFx in F_1 ligands electrostatically to β Arg-246 in wild type, and the Lys mutation provides the same liganding. Whether the complex represents a ground state, catalytic intermediate, or dead-end complex is unclear. An x-ray structure of MgADP·BeFx trapped in F_1 catalytic sites has not yet been published. Further interpretation of our results will have to await structural analysis.

All three mutants rendered F_1 insensitive to azide inhibition. In mitochondrial and *Bacillus* PS3 enzymes, azide is thought to inhibit by trapping MgADP at catalytic sites, possibly by acting as a P_i analog in a tightly bound MgADP· N_3^- complex (46). However, in *E. coli* F_1 this did not seem to be the case (45), rather it was suggested that azide interfered with conformational signal transmission between catalytic sites required for rapid catalysis. It had been suggested previously (51) that residue β Arg-246 is responsible for such conformational signaling. If signaling is already defunct in the mutant enzymes, with resultant low ATPase, then further inhibition by azide might not be expected. Thus the data do not necessarily support a direct role for β Arg-246 in P_i binding. However, they do reaffirm that the residual ATPase activity seen in the mutant enzymes is going via a different catalytic pathway to normal.

NBD-Cl inhibited the ATPase activity of the mutant enzymes to only ~50%, at full reaction, as compared with essentially 100% in wild type, providing further evidence that the ATPase of the mutants is different in character from wild type. NBD-Cl still reacted with β Tyr-297 in the mutants as in wild type. Somewhat higher concentrations of NBD-Cl were required for inhibition in the mutants. As noted in Fig. 1, residue β Arg-246 is close to β Tyr-297 in wild-type catalytic sites. Orriss *et al.* (47) have concluded from their x-ray crystallography studies that NBD-Cl reacts only in the empty (β E) catalytic site of wild-type enzyme. Our data support the conclusion that the rate of inactivation was linearly dependent on NBD-Cl concentration and only very high concentrations of MgADP gave protection from reaction. We presume that the high concentrations of MgADP are needed in order to keep the β E site inaccessible to NBD-Cl in the time average. Because the same very high concentrations of MgADP were required to protect the mutant enzymes from inhibition, the same conclusion applies to the mutants.

The protection that P_i afforded against NBD-Cl inhibition in wild-type membranes and purified F_1 is of great interest, because it shows that the presence of P_i in the β E site, probably in a position similar to that of SO_4^{2-} in the " β ADP + P_i " site (Fig. 1D), impedes accessibility and/or reaction of NBD-Cl with β Tyr-297. Perez *et al.* (48) favored the interpretation that pro-

tection was due to P_i binding in catalytic sites, but they were not yet in possession of structural information that now solidifies this conclusion and also makes it clear which particular catalytic site conformation is involved. Moreover, no protection by P_i was seen here in any of the mutants, providing evidence that P_i binding was to the β Arg-246 side chain in the β E site.

Earlier work from our laboratory (7) reported that in aqueous buffer at pH 6.5–7.5 maximal stoichiometry of [32 P] P_i binding to wild-type *E. coli* F_1 measured using the centrifuge column technique (54) was 0.125 mol/mol after incubation with 1 mM P_i . It should be noted that the radioactive P_i was first purified to remove PP_i and higher polyphosphates, as described previously (55, 56), and that this precaution reduced the amount of F_1 -bound radioactivity considerably. (Subsequent experiments have shown that PP_i (10) and PPP_i (18) bind with K_d of 20 and 50 μM to the noncatalytic sites of *E. coli* F_1 .) Penefsky (54) showed that under the conditions used for centrifuge column elution, the transit time for protein is around 30 s, so that for ~90% retention of bound ligand a dissociation rate $\leq 0.006 \text{ s}^{-1}$ would be required. As was pointed out in Ref. 7, P_i bound in the highest affinity catalytic site should be retained in centrifuge column experiments, as determined from unisite kinetics of P_i release. It is, however, quite feasible that P_i bound in the β E site would have a dissociation constant sufficiently fast that it would not be retained upon centrifuge column elution. Consistent with this, Perez *et al.* (48) calculated a $K_d P_i$ of 0.2 mM from kinetic experiments involving inactivation of mitochondrial membrane ATPase by NBD-Cl at varied P_i concentration. Our experimental data with *E. coli* enzyme (Fig. 8) are similar.

We also found earlier that binding of Mg-AMPPNP or ATP (no Mg^{2+}) to the three catalytic sites of *E. coli* F_1 was not competed by 5 mM P_i (8, 9), from which we concluded that the $K_d P_i$ at all three of the catalytic sites was $\geq 10 \text{ mM}$ (10). Results discussed above indicate that the β E site does bind P_i , with K_d in the mM range. It is possible that, in the absence of rotation, a β E site with P_i bound can partly close and still accommodate P_i along with Mg-AMPPNP or ATP, so that competition between these ligands is not evident. Presumably during rotational catalysis induced by MgATP, any P_i bound along with MgATP in β E is expelled as full closing of the site occurs, and P_i in the medium cannot access fully closed sites. This would be consistent with the well established lack of inhibition of ATPase by P_i (*e.g.* Ref. 57 found no inhibition at 50 mM P_i). In contrast, in proton gradient-driven rotation, P_i bound to β E must be retained as the site closes. How this is achieved is not yet established; however, the work presented here clearly shows that the β Arg-246 side chain is an important component in binding P_i and in forming the transition state.

Acknowledgments—We thank Erich Huang for outstanding technical assistance and Dr. Sashi Nadanaciva for construction of plasmid pSN6.

REFERENCES

- Weber, J., and Senior, A. E. (2003) *FEBS Lett.* **545**, 61–70
- Senior, A. E., Nadanaciva, S., and Weber, J. (2002) *Biochim. Biophys. Acta* **1553**, 188–211
- Noji, H., and Yoshida, M. (2001) *J. Biol. Chem.* **276**, 1665–1668
- Leslie, A. G. W., and Walker, J. E. (2000) *Phil. Trans. R. Soc. Lond. B Biol. Sci.* **355**, 465–472
- Rosing, J., Kayalar, C., and Boyer, P. D. (1977) *J. Biol. Chem.* **252**, 2478–2485
- Boyer, P. D. (1989) *FASEB J.* **3**, 2164–2178
- Al-Shawi, M. K., and Senior, A. E. (1992) *Biochemistry* **31**, 886–891
- Weber, J., Wilke-Mounts, S., Lee, R. S. F., Grell, E., and Senior, A. E. (1993) *J. Biol. Chem.* **268**, 20126–20133
- Löbau, S., Weber, J., and Senior, A. E. (1998) *Biochemistry* **37**, 10846–10853
- Weber, J., and Senior, A. E. (1995) *J. Biol. Chem.* **270**, 12653–12658
- Al-Shawi, M. K., Parsonage, D., and Senior, A. E. (1989) *J. Biol. Chem.* **264**, 15376–15383
- Wise, J. G., and Senior, A. E. (1985) *Biochemistry* **24**, 6949–6954
- Al-Shawi, M. K., Ketchum, C. J., and Nakamoto, R. K. (1997) *Biochemistry* **36**, 12961–12969
- Fischer, S., Etzold, C., Turina, P., Deckers-Hebestreit, G., Altendorf, K., and

- Gräber, P. (1994) *Eur. J. Biochem.* **225**, 167–172
15. Masaike, T., Muneyuki, E., Noji, H., Kinoshita, K., and Yoshida, M. (2002) *J. Biol. Chem.* **277**, 21643–21649
16. Weber, J., Hammond, S. T., Wilke-Mounts, S., and Senior, A. E. (1998) *Biochemistry* **37**, 608–614
17. Dou, C., Fortes, P. A. G., and Allison, W. S. (1998) *Biochemistry* **37**, 16757–16764
18. Weber, J., and Senior, A. E. (2000) *Biochim. Biophys. Acta* **1458**, 300–309
19. Menz, R. I., Walker, J. E., and Leslie, A. G. W. (2001) *Cell* **106**, 331–341
20. Braig, K., Menz, R. I., Montgomery, M. G., Leslie, A. G. W., and Walker, J. E. (2000) *Structure (Lond.)* **8**, 567–573
21. Noumi, T., Taniai, M., Kanazawa, H., and Futai, M. (1986) *J. Biol. Chem.* **261**, 9196–9201
22. Parsonage, D., Duncan, T. M., Wilke-Mounts, S., Kironde, F. A. S., Hatch, L., and Senior, A. E. (1987) *J. Biol. Chem.* **262**, 6301–6307
23. Bockmann, R. A., and Grubmüller, H. (2002) *Nat. Struct. Biol.* **9**, 198–202
24. Yang, W., Gao, Y. Q., Cui, Q., Ma, J., and Karplus, M. (2003) *Proc. Natl. Acad. Sci. U. S. A.* **100**, 874–879
25. Dittrich, M., Hayashi, S., and Schulten, K. (2003) *Biophys. J.* **85**, 2253–2266
26. Senior, A. E., Langman, L., Cox, G. B., and Gibson, F. (1983) *Biochem. J.* **210**, 395–403
27. Weber, J., Lee, R. S. F., Grell, E., Wise, J. G., and Senior, A. E. (1992) *J. Biol. Chem.* **267**, 1712–1718
28. Senior, A. E., Latchney, L. R., Ferguson, A. M., and Wise, J. G. (1984) *Arch. Biochem. Biophys.* **228**, 49–53
29. Taussky, H. H., and Shorr, E. (1953) *J. Biol. Chem.* **202**, 675–685
30. Rao, R., Al-Shawi, M. K., and Senior, A. E. (1988) *J. Biol. Chem.* **263**, 5569–5573
31. Ketchum, C. J., Al-Shawi, M. K., and Nakamoto, R. K. (1998) *Biochem. J.* **330**, 707–712
32. Vandeyar, M., Weiner, M., Hutton, C., and Batt, C. (1988) *Gene (Amst.)* **65**, 129–133
33. Klionsky, D. J., Brusilow, W. S. A., and Simoni, R. D. (1984) *J. Bacteriol.* **160**, 1055–1060
34. Weber, J., and Senior, A. E. (2004) *Methods Enzymol.* **380**, 132–152
35. Lobau, S., Weber, J., Wilke-Mounts, S., and Senior, A. E. (1997) *J. Biol. Chem.* **272**, 3648–3656
36. Goodno, C. C. (1982) *Methods Enzymol.* **85**, 116–123
37. Lunardi, J., Dupuis, A., Garin, J., Issartel, J. P., Michel, L., Chabre, M., and Vignais, P. V. (1988) *Proc. Natl. Acad. Sci. U. S. A.* **85**, 8958–8962
38. Nadanaciva, S., Weber, J., and Senior, A. E. (1998) *J. Biol. Chem.* **274**, 7052–7058
39. Nadanaciva, S., Weber, J., and Senior, A. E. (1999) *Biochemistry* **38**, 7670–7677
40. Nadanaciva, S., Weber, J., and Senior, A. E. (1999) *Biochemistry* **38**, 15493–15499
41. Nadanaciva, S., Weber, J., and Senior, A. E. (2000) *Biochemistry* **39**, 9583–9590
42. Smith, C. A., and Rayment, I. (1996) *Biochemistry* **35**, 5404–5417
43. Lahiri, S. D., Zhang, G., Dunaway-Mariano, D., and Allen, K. N. (2003) *Science* **299**, 2067–2071
44. Fisher, A. J., Smith, C. A., Thoden, J. B., Smith, R., Sutoh, K., Holden, H. M., and Rayment, I. (1995) *Biochemistry* **34**, 8960–8972
45. Weber, J., and Senior, A. E. (1998) *J. Biol. Chem.* **273**, 33210–33215
46. Dou, C., Grodsky, N. B., Matsui, T., Yoshida, M., and Allison, W. S. (1997) *Biochemistry* **36**, 3719–3727
47. Orriss, G. L., Leslie, A. G. W., Braig, K., and Walker, J. E. (1998) *Structure (Lond.)* **6**, 831–837
48. Perez, J. A., Greenfield, A. J., Sutton, R., and Ferguson, S. J. (1986) *FEBS Lett.* **198**, 113–118
49. Ferguson, S. J., Lloyd, W. J., Lyons, M. H., and Radda, G. K. (1975) *Eur. J. Biochem.* **54**, 117–126
50. Ferguson, S. J., Lloyd, W. J., and Radda, G. K. (1975) *Eur. J. Biochem.* **54**, 127–133
51. Al-Shawi, M. K., Parsonage, D., and Senior, A. E. (1990) *J. Biol. Chem.* **265**, 4402–4410
52. Xu, Y. W., Morera, S., Janin, J., and Cherfils, J. (1997) *Proc. Natl. Acad. Sci. U. S. A.* **94**, 3579–3583
53. Schlichting, I., and Reinstein, J. (1997) *Biochemistry* **36**, 9290–9296
54. Penefsky, H. S. (1977) *J. Biol. Chem.* **252**, 2891–2899
55. Kanazawa, T., and Boyer, P. D. (1973) *J. Biol. Chem.* **248**, 3163–3170
56. DeMeis, L., and Tume, R. K. (1977) *Biochemistry* **16**, 4455–4463
57. DeMeis, L. (1987) *FEBS Lett.* **213**, 333–336